Vol 18 No 12, December 2009
1674-1056/2009/18(12)/5155-06

Chinese Physics B

© 2009 Chin. Phys. Soc.
and IOP Publishing Ltd

Quantum information procession with fermions based on charge detection

Tang Li(唐 莉)†

Hefei National Laboratory for Physical Sciences at Microscale and Department of Modern Physics, University of Science and Technology of China, Hefei 230026, *China*

(Received 18 September 2008; revised manuscript received 16 December 2008)

This paper proposes a fermionic linear optical scheme for the teleportation and entanglement concentration via entanglement swapping based on charge detection. It also proves that this method is useful in generating entangled states such as GHZ states, W states, and cluster states by using fermionic polarizing beam splitters and single spin rotations assisted by a parity check on the fermionic qubits. This scheme is nearly deterministic (i.e., with 100% successful probability) and does not need the joint Bell state measurement required in the previous schemes.

Keywords: quantum information processing，charge detection
PACC: 0367, 0365, 4250

Over the course of the past century, quantum information processing (QIP) has been investigated quite extensively and deeply. A growing amount of interest in studying the implementation of QIP tasks has appeared in recent literatures. Among the typical QIP tasks such as quantum teleportation[1] and quantum swapping,[2] a certain user always needs to operate a joint Bell-state measurement[3,4] on the two particles possessed by him. Thus the joint Bell-state measurement plays an important role in QIP. This paper proposes a new scheme for the teleportation and entanglement concentration via entanglement swapping based on charge detection, which overcomes the empirical difficulties found in joint measurement. It is also proved that this method is useful in generating entangled states such as GHZ (Greenberger–Horne–Zeilinger) states,[5] W states[6] and cluster states.[7]

It is known that the electron carrying the qubit in its spin degree of freedom also has a charge degree of freedom. Since spin and charge commute, a measurement of the charge leaves the spin qubit unaffected.[8] Since the previous no-go theorem[9,10] stated that, the operators with fermionic beam splitters and single-spin rotations cannot achieve universal quantum computation in free fermion systems as that in bosons, this strongly holds back the search for free fermionic quantum computation. However, earlier works[8,11] showed that assisted by charge detectors a CNOT (controlled NOT) gate and partial Bell-state measurements for fermions are possible in principle. In Ref.[8], the general formulation of fermionic quantum computation is proposed and a CNOT gate is constructed by using only fermionic beam splitters, spin rotations and charge detectors. Since the CNOT gate is a universal quantum gate,[12] partial Bell-state measurements and single-qubit operations are sufficient to build a universal quantum computer.

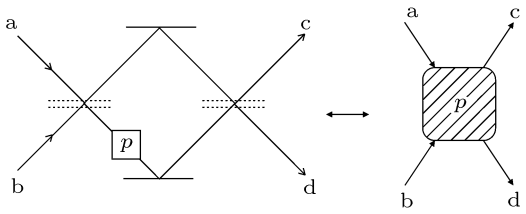


Fig.1. Encoders designed in Ref.[8]. A polarizing beam splitter (double dashed line) transmits spin up and reflects spin down. A charge detector (squares) records bunching ($p = 0$) or antibunching ($p = 1$) and passes the electrons on to a second polarizing beam splitter. The shaded box at the right represents the circuit shown at the left. The gate could operate as a parity meter, convert a charge measurement to a spin parity measurement, measuring $p = 1$ (if the two spins are arrayed) or $p = 0$ (if they are opposite), especially could entangle the input state $\alpha|0\rangle + \beta|1\rangle$ encoded in arm a and an ancilla's state $(|0\rangle + |1\rangle)/\sqrt{2}$ encoded in arm b into $\alpha|0\rangle|0\rangle + \beta|1\rangle|1\rangle$ for $p = 1$, or $\alpha|0\rangle|1\rangle + \beta|1\rangle|0\rangle$ for $p = 0$. Here we denote spin up by $|0\rangle$ and spin down by $|1\rangle$.

Firstly we will provide a brief background on the charge detector called an encoder. As depicted in Fig.1, the device consists of two fermionic polarizing beam splitters in series, with the charge detector in between. A polarizing beam splitter fully transmits $|0\rangle$ and fully reflects $|1\rangle$. At the input two electrons

†Corresponding author. E-mail: litang@mail.ustc.edu.cn

are incident in different arms. Input equals output if each electron is in a spin eigenstate. The measured charge parity then records whether the two spins are the same or opposite.

Before proceeding, we note that the probabilistic CNOT gate using linear optical elements is well studied. In Refs.[13]–[15] it was demonstrated that a probabilistic CNOT gate could be implemented by using a modified form of quantum teleportation and a four-qubit entanglement state $|\chi\rangle = (|HHHH\rangle + |HVHV\rangle + |VHVV\rangle + |VVVH\rangle)/2$ as a resource (ancilla), assisted by partial Bell-state measurement (consists of one-and-only-one detections of the output). The CNOT gate will give the desired result with certainty when a specific output from the detectors is obtained. Using polarizing beam splitters and a quantum erasure technique, we can increase the probability of success from 1/16 to 1/4. Later, Pittman *et al* in Ref.[16] proposed an alternative approach to construct the probabilistic CNOT gate which eliminates the teleportation and replaces two of the ancillas with the actual input qubits. The probabilistic CNOT gate could be constructed by combining a quantum encoder with a destructive CNOT using polarizing splitters and two ancillas. The operation is successful with certainty when the specified combination of detectors each registers a single photon. Since the quantum parity check and destructive CNOT operations both succeed with a probability of 1/2, it follows that the CNOT gate will succeed with an overall probability of 1/4.

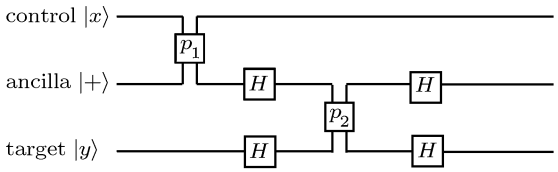


Fig.2. Deterministic CNOT gate consists of two encoders depicted in Fig.1 and four Hadamard gates $H = (\sigma_x + \sigma_z)/\sqrt{2}$. At the output, the spin of the ancilla qubit is measured (assumed that the measured value is z). According to the two measured parities p_1, p_2 of the two encoders P_1, P_2 and the outcome z, we decide whether to perform a Pauli operator σ_z or σ_x on the control and target bit respectively.

In contrast to the design using polarized photons in Ref.[16] with successful probability of 1/4, the CNOT gate in our scheme is deterministic (i.e., with 100% successful probability) using only one ancilla, and does not need the joint Bell state measurement required in the previous schemes, i.e. the joint Bell-state measurement has been converted into the product of separate measurements on single fermions.

The deterministic CNOT gate using the encoder is illustrated in Fig.2, which requires one ancilla in $|+\rangle = (|0\rangle + |1\rangle)/\sqrt{2}$ to achieve 100% successful probability. At the input the control qubit is $|x\rangle$, the target qubit is $|y\rangle$, with $x, y \in \{0, 1\}$. The effect of the first encoder P_1 is given by

$$|x\rangle|+\rangle \longrightarrow \begin{cases} |00\rangle & x = 0,\ p_1 = 1, \\ |11\rangle & x = 1,\ p_1 = 1, \\ |01\rangle & x = 0,\ p_1 = 0, \\ |10\rangle & x = 1,\ p_1 = 0, \end{cases} \tag{1}$$

which can be rewritten as

$$|x\rangle|+\rangle \longrightarrow |x\rangle|x + p_1 + 1\rangle. \tag{2}$$

Here the additions are assumed to be module 2 and p_1 is the parity measured by the encoder P_1. In the following we will omit normalization constants for simplicity.

As we know, the Hadamard gate transforms the state of the input qubit $|a\rangle$ ($a \in \{0, 1\}$) into

$$|a\rangle \longrightarrow (|0\rangle + (-1)^a|1\rangle). \tag{3}$$

After the Hadamard gate applies to the ancilla qubit (denoted by $|x + p_1 + 1\rangle$) and target qubit (denoted by $|y\rangle$) respectively, based on Eq.(3), the whole state of the system becomes

$$|\Psi\rangle = |x\rangle(|0\rangle + (-1)^{x+p_1+1}|1\rangle)(|0\rangle + (-1)^y|1\rangle). \tag{4}$$

When the ancilla and target qubit pass through the second encoder P_2, the whole state $|\Psi\rangle$ evolves in the form ($p_2 = 1$)

$$|\Psi\rangle_1 = |x\rangle[(-1)^{x+p_1+1+y}|1\rangle|1\rangle + |0\rangle|0\rangle], \tag{5}$$

or in the form ($p_2 = 0$)

$$|\Psi\rangle_0 = |x\rangle[(-1)^y|0\rangle|1\rangle + (-1)^{x+p_1+1}|1\rangle|0\rangle]. \tag{6}$$

Then the Hadamard gates perform the last transformation to the whole state as follows:

$$|\Psi\rangle_1 \longrightarrow |x\rangle(|0\rangle|x + p_1 + 1 + y\rangle + |1\rangle|x + p_1 + y\rangle), \tag{7}$$

and

$$|\Psi\rangle_0 \longrightarrow (-1)^{x+p_1+1}|x\rangle(|0\rangle|x + p_1 + 1 + y\rangle - |1\rangle|x + p_1 + y\rangle). \tag{8}$$

At the output, the spin of the ancilla qubit is measured (assumed that the measured value is z), the state of the control and target qubit $|\Psi\rangle_{\rm out}$ is depicted in Table 1.

Table 1. The final state of the control and target qubit $|\Psi\rangle_{\rm out}$ versus z and p_2.

z	p_2	$\|\Psi\rangle_{\rm out}$
0	0	$(-1)^{x+p_1+1}\|x\rangle\|x+p_1+1+y\rangle$
0	1	$\|x\rangle\|x+p_1+1+y\rangle$
1	0	$(-1)^{x+p_1}\|x\rangle\|x+p_1+y\rangle$
1	1	$\|x\rangle\|x+p_1+y\rangle$

It is noticed that $|\Psi\rangle_{\rm out}$ can be rewritten in a more compact form

$$|\Psi\rangle_{\rm out}=(-1)^{(x+p_1+1+z)(p_2+1)}|x\rangle|x+p_1+1+y+z\rangle. \tag{9}$$

The phase factor term can be written as $\phi=\phi_1+\phi_2$, where $\phi_1=(-1)^{(p_1+1+z)(p_2+1)}$ and $\phi_2=(-1)^{(p_2+1)x}$. Since p_1, p_2, z are independent of the input, ϕ_1 can be ignored without any trouble. To eliminate the effect of ϕ_2, we may perform a σ_z operation on the control qubit $|x\rangle$ (since $\sigma_z|x\rangle=(-1)^x|x\rangle$) when $p_2=0$. No operation is performed on the control qubit if $p_2=1$. Analogously, performing a σ_x operation on the target qubit when $z+p_1=0$ will transform $|x+p_1+1+y+z\rangle$ to the required result $|x+y\rangle$. See more details are listed in Table 2.

Table 2. Arrangement of the Pauli operations performed on the control and target qubit according to p_1, p_2 and z.

p_1	p_2	z	control quit	target qubit
0	0	0	σ_z	σ_x
0	0	1	σ_z	I
0	1	0	I	σ_x
0	1	1	I	I
1	0	0	σ_z	I
1	0	1	σ_z	σ_x
1	1	0	I	I
1	1	1	I	σ_x

Let us see how the encoders could apply to the teleportation of electrons. The state to be teleported is $|\phi\rangle=\alpha|0\rangle+\beta|1\rangle$, where α and β are unknown amplitudes. Before the teleportation, the sender (Alice) and the receiver (Bob) share the EPR state

$$|{\rm EPR}\rangle_{23}=\frac{1}{\sqrt{2}}(|00\rangle_{23}+|11\rangle_{23}), \tag{10}$$

where Alice possesses electrons 1, 2 and Bob possesses electron 3. To complete the teleportation of the unknown state of electron 1, only one encoder will be introduced at Alice's location. The main setup of our scheme is depicted in Fig.3. The effect of the encoder on the input electrons can be expressed as

$$\begin{aligned}|\Phi\rangle&=(\alpha|0\rangle_1+\beta|1\rangle_1)(|00\rangle_{23}+|11\rangle_{23})\\&\longrightarrow\begin{cases}\alpha|000\rangle_{123}+\beta|111\rangle_{123}, & p=1,\\ \alpha|011\rangle_{123}+\beta|100\rangle_{123}, & p=0.\end{cases}\end{aligned} \tag{11}$$

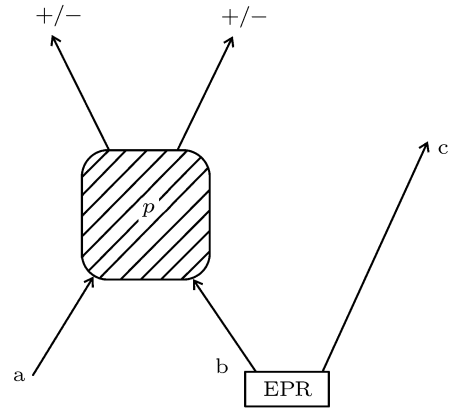


Fig.3. The setup for the teleportation scheme. Alice places electrons 1, 2 to the input arms a and b respectively. After Alice performs $+/-$ measurements in the bases $\{|+\rangle,|-\rangle\}$ ($|\pm\rangle=(|0\rangle\pm|1\rangle)/\sqrt{2}$), electron 3 possessed by Bob will collapse to the required state.

If Alice performs $+/-$ measurements in the bases $\{|+\rangle,|-\rangle\}$, Bob's system will be in the state $|\phi\rangle$ (up to unitary equivalence). We can read off Bob's post measurement state which gives the result of Alice' measurement as follows:

$$\begin{aligned}|++\rangle_{12}&\longrightarrow\begin{cases}|\Psi\rangle_3=\alpha|0\rangle_3+\beta|1\rangle_3, & p=1,\\ |\Psi\rangle_3=\alpha|1\rangle_3+\beta|0\rangle_3, & p=0,\end{cases}\\ |--\rangle_{12}&\longrightarrow\begin{cases}|\Psi\rangle_3=\ \alpha|0\rangle_3+\beta|1\rangle_3, & p=1,\\ |\Psi\rangle_3=-\alpha|1\rangle_3-\beta|0\rangle_3, & p=0,\end{cases}\\ |+-\rangle_{12}&\longrightarrow\begin{cases}|\Psi\rangle_3=\ \alpha|0\rangle_3-\beta|1\rangle_3, & p=1,\\ |\Psi\rangle_3=-\alpha|1\rangle_3+\beta|0\rangle_3, & p=0,\end{cases}\\ |-+\rangle_{12}&\longrightarrow\begin{cases}|\Psi\rangle_3=\alpha|0\rangle_3-\beta|1\rangle_3, & p=1,\\ |\Psi\rangle_3=\alpha|1\rangle_3-\beta|0\rangle_3, & p=0.\end{cases}\end{aligned} \tag{12}$$

Depending on Alice's measurement outcome, Bob's system will be ended up in one of the above states. With the Pauli operations of I, σ_x, σ_y or σ_z, the state of electron 3 will be left in the required state $|\phi\rangle$.

Now we continue to discuss the implementation of entanglement concentration via entanglement swapping[17] assisted by an encoder. Suppose there

are three spatially separate users Alice, Bob and Cliff. Alice and Bob all share a pair of non-maximally entangled electrons with Cliff. Alice possesses electron 1, Bob possesses electron 4, and electrons 2, 3 are all at Cliff's location. Figure 4 prepares the initially state as

$$|\Phi\rangle_{12} = \alpha|0\rangle_1|0\rangle_2 + \beta|1\rangle_1|1\rangle_2,$$
$$|\Phi\rangle_{34} = a|0\rangle_3|0\rangle_4 + b|1\rangle_3|1\rangle_4, \tag{13}$$

where α, β, a, b are normalization coefficients.

Before swapping, the state of the total system can be expressed as

$$|\Phi\rangle = (\alpha|0\rangle_1|0\rangle_2 + \beta|1\rangle_1|1\rangle_2)(a|0\rangle_3|0\rangle_4 + b|1\rangle_3|1\rangle_4)$$
$$\longrightarrow \begin{cases} \alpha a|0000\rangle_{1234} + \beta b|1111\rangle_{1234}, & p = 1, \\ \alpha b|0011\rangle_{1234} + \beta a|1100\rangle_{1234}, & p = 0. \end{cases} \tag{14}$$

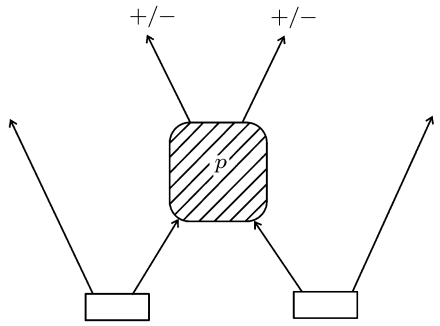


Fig.4. The setup for the entanglement concentration via entanglement swapping.

After Cliff performs $+/-$ measurements, the state of the total system will be

$$|++\rangle_{23} \longrightarrow \begin{cases} \alpha a|00\rangle_{14} + \beta b|11\rangle_{14}, & p = 1, \\ \alpha b|01\rangle_{14} + \beta a|10\rangle_{14}, & p = 0, \end{cases} \tag{15a}$$

$$|--\rangle_{23} \longrightarrow \begin{cases} \alpha a|00\rangle_{14} + \beta b|11\rangle_{14}, & p = 1, \\ -\alpha b|01\rangle_{14} - \beta a|10\rangle_{14}, & p = 0, \end{cases} \tag{15b}$$

$$|+-\rangle_{23} \longrightarrow \begin{cases} \alpha a|00\rangle_{14} - \beta b|11\rangle_{14}, & p = 1, \\ -\alpha b|01\rangle_{14} + \beta a|10\rangle_{14}, & p = 0, \end{cases} \tag{15c}$$

$$|-+\rangle_{23} \longrightarrow \begin{cases} \alpha a|00\rangle_{14} - \beta b|11\rangle_{14}, & p = 1, \\ \alpha b|01\rangle_{14} - \beta a|10\rangle_{14}, & p = 0. \end{cases} \tag{15d}$$

If we set $\alpha a = \beta b$ or $\alpha b = \beta a$, the above states will become maximally entangled states. For example, $\alpha = b$, $\beta = a$ or $\alpha = a$, $\beta = b$. Therefore the initial non-maximally entangled states have been concentrated into maximally entangled states via entanglement swapping.

In what follows, we will show that the method could also be generalized to construct entangled states such as GHZ states, W states and cluster states assisted by encoders. As we know, the encoder can deterministically entangle a qubit in the arbitrary state $\alpha|0\rangle + \beta|1\rangle$ and an ancilla in the fixed state $(|0\rangle + |1\rangle)/\sqrt{2}$ into the two-particle entangled state $\alpha|0\rangle|0\rangle + \beta|1\rangle|1\rangle$. The generation of N-electron GHZ states can be deduced by analogy of Fig.3.

Based on the CNOT gate using the encoder depicted in Fig.2, we could realize a W state as follows. We consider three non-interacting electrons in Fig.5 prepared initially in $|0\rangle|0\rangle|0\rangle$. After three single-qubit operations H, U_1, U_2 are performed on them respectively, the state of the total system becomes

$$|\Phi\rangle = |\phi\rangle_1|\phi\rangle_2|\phi\rangle_3, \tag{16}$$

where

$$|\phi\rangle_1 = \frac{1}{\sqrt{2}}(|0\rangle_1 + |1\rangle_1),$$
$$|\phi\rangle_2 = \frac{1}{\sqrt{3}}(|0\rangle_2 + \sqrt{2}|1\rangle_2),$$
$$|\phi\rangle_3 = \cos\frac{\pi}{8}|0\rangle_3 + \sin\frac{\pi}{8}|1\rangle_3. \tag{17}$$

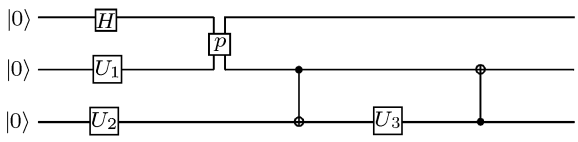


Fig.5. Network generating the W state.

When $p = 0$, the whole system will collapse to

$$|\Phi\rangle = \frac{1}{\sqrt{3}}(\sqrt{2}|01\rangle_{12} + |10\rangle_{12})|\phi\rangle_3. \tag{18}$$

After two CNOT gates and a single-qubit operation U_3 are performed, it is easy to verify that the W state can be created by the network presented in Fig.5

$$
\begin{aligned}
|\Phi\rangle &\xrightarrow{\text{CNOT}} \frac{1}{\sqrt{3}}\Big(\sqrt{2}\cos\frac{\pi}{8}|011\rangle_{123}+\sqrt{2}\sin\frac{\pi}{8}|010\rangle_{123} \\
&\quad +\cos\frac{\pi}{8}|100\rangle_{123}+\sin\frac{\pi}{8}|101\rangle_{123}\Big) \\
&\xrightarrow{U_3} \frac{1}{\sqrt{3}}(|010\rangle_{123}+|011\rangle_{123}+|100\rangle_{123}) \\
&\xrightarrow{\text{CNOT}} \frac{1}{\sqrt{3}}(|010\rangle_{123}+|001\rangle_{123}+|100\rangle_{123}).
\end{aligned} \tag{19}
$$

When $p=1$, the whole system will collapse to $|\Phi\rangle' = (|000\rangle_{123}+|110\rangle_{123}+|101\rangle_{123})/\sqrt{3}$. Performing a σ_x operation on qubit 1 will transform $|\Phi\rangle'$ to the required result.

Here H denotes the standard Hadamard gate and is given by

$$
H=\frac{1}{\sqrt{2}}\begin{pmatrix}1 & 1\\ 1 & -1\end{pmatrix}, \tag{20}
$$

and the unitary operations U_1, U_2 and U_3 appearing in Fig.5 take the form

$$
U_1=\frac{1}{\sqrt{3}}\begin{pmatrix}1 & -\sqrt{2}\\ \sqrt{2} & 1\end{pmatrix}, \tag{21}
$$

$$
U_2=\begin{pmatrix}\cos\frac{\pi}{8} & -\sin\frac{\pi}{8}\\ \sin\frac{\pi}{8} & \cos\frac{\pi}{8}\end{pmatrix}, \tag{22}
$$

$$
U_3=\begin{pmatrix}\cos\frac{\pi}{8} & \sin\frac{\pi}{8}\\ -\sin\frac{\pi}{8} & \cos\frac{\pi}{8}\end{pmatrix}. \tag{23}
$$

Cluster states regarded as a special type of multiparticle entangled states serve as the universal basis for quantum computation in the one-way quantum computation.[7,18,19] Moreover, they are widely used in the quantum error-correction code[20] and the test of quantum nonlocality.[21] There have been a number of experimental systems proposed as candidates for the generation of cluster states, and several of them have been implemented, e.g., creation of six-photon cluster states with verifiable six-partite entanglement by a linear optical elements.[22]

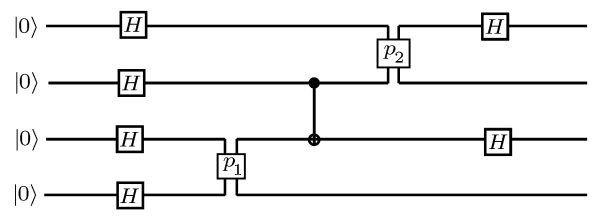


Fig.6. Network generating the cluster state $|\phi_4\rangle$.

We could construct the network (depicted in Fig.6) to realize a cluster state $|\phi_4\rangle = (|+\rangle|0\rangle|+\rangle|0\rangle + |+\rangle|0\rangle|-\rangle|1\rangle + |-\rangle|1\rangle|-\rangle|0\rangle + |-\rangle|1\rangle|+\rangle|1\rangle)/2$, composed of six Hadamard gates, two encoders and a CNOT gate depicted in Fig.2. The evolution can be written as follows:

$$
\begin{aligned}
&|0000\rangle \\
&\xrightarrow{H} |+\rangle|+\rangle|+\rangle|+\rangle \\
&\xrightarrow{p_1=1} |+\rangle|+\rangle(|0\rangle|0\rangle+|1\rangle|1\rangle) \\
&\xrightarrow{\text{CNOT}} |+\rangle[|0\rangle(|0\rangle|0\rangle+|1\rangle|1\rangle)+|1\rangle(|1\rangle|0\rangle+|0\rangle|1\rangle)] \\
&\xrightarrow{p_2=1} |0\rangle|0\rangle(|0\rangle|0\rangle+|1\rangle|1\rangle)+|1\rangle|1\rangle(|1\rangle|0\rangle+|0\rangle|1\rangle) \\
&\xrightarrow{H} |\phi_4\rangle.
\end{aligned} \tag{24}
$$

Assisted by the Pauli operations σ_z, σ_x performed on qubit 1 or 2 according to the two measured parities p_1, p_2, we will transform the final state of the network to the required result $|\phi_4\rangle$. See more details in Table 3.

Table 3. Arrangement of the Pauli operations performed on qubits 1 and 2 according to p_1 and p_2.

p_1	p_2	operation
0	0	σ_x^2
0	1	$\sigma_z^1\sigma_x^2$
1	0	σ_z^1
1	1	I

In summary, we proposed a fermionic linear optical scheme for the teleportation and entanglement concentration via entanglement swapping based on charge detection. We also prove that this method is useful in generating entangled states such as GHZ states, W states and cluster states using fermionic polarizing beam splitters and single spin rotations assisted by a parity check on the fermionic qubits. Our scheme is nearly deterministic (i.e., with 100% successful probability) and does not need the joint Bell state measurement required in the previous schemes, i.e. the joint Bell-state measurement has been converted into the product of separate measurements on single fermions.

Although the fermionic parity detector such as the electronic parity detector studied here has not yet been realized experimentally, the fermionic beam splitters such as electronic beam splitters[23,24] and the charge detectors[25–27] needed in our scheme have both been realized by means of point contacts in a two-dimensional electron gas. The mesoscopic electron beam splitter could be realized by a lithographically patterned metallic split gate (light shading)[23]

or formed monolithically by a 40-nm finger, with the splitting ratio tuned by applying a small bias voltage to this finger.[24] As to charge detection, one method was proposed and realized in metal(Al)tunnel junctions by Lafarge,[25] where a single electron transistor (SET) was used to detect charge in a single electron box. The advantage of this method lies in the sensitivity of the SET to the presence of charge near the SET island. Other charge detection methods have been proposed and investigated in AlGaAs/GaAs materials.[26,27] Field *et al*[26] demonstrated a "noninvasive" detector for measuring the electrostatic potential change on a quantum dot. This method of charge detection is considered as noninvasive, since the constriction (one-dimensional channel) has a negligible effect on the behaviour of the quantum dot. With the potential application of fermionic quantum computing as well as rapid development of quantum dot techniques, we hope that our analysis could offer advice for experimenters and be testified by experiment in the near future.

Acknowledgement

The author is grateful to professor Chen Zeng-Bing for critically reading the manuscript and helpful suggestions.

References

[1] Bennett C H, Brassard G, Crépeau C, Jozsa R, Peres A and Wootters W K 1993 *Phys. Rev. Lett.* **70** 1895
[2] Żukowski M, Zeilinger A, Horne M A and Ekert A K 1993 *Phys. Rev. Lett.* **71** 4287
[3] Lütkenhaus N, Calsamiglia J and Suominen K A 1999 *Phys. Rev.* A **59** 3295
[4] Vaidman L and Yoran N 1999 *Phys. Rev.* A **59** 116
[5] Greenberger D M, Horne M A, Shimony A and Zeilinger A 1990 *Am. J. Phys.* **58** 1131
Mermin N D 1990 *Am. J. Phys.* **58** 731
[6] Dür W, Vidal G and Cirac J I 2000 *Phys. Rev.* A **62** 062314
[7] Briegel H J and Raussendorf R 2001 *Phys. Rev. Lett.* **86** 910
Zhang J, Zhou X Q and Yang T 2007 *Chin. Phys.* **16** 2224
Zhou X Q and Yang T 2008 *Chin. Phys.* B **17** 3549
[8] Beenakker C W J, DiVincenzo D P, Emary C and Kindermann M 2004 *Phys. Rev. Lett.* **93** 020501
[9] Terhal B M and DiVincenzo D P 2002 *Phys. Rev.* A **65** 032325
[10] Knill E 2001 quant-ph/0108033V2
[11] Bravyi S B and Kitaev A Y 2000 quant-ph/0003137V2
[12] Barenco A, Bennett C H, Cleve R, DiVincenzo D P, Margolus N, Shor P, Sleator T, Smolin J A and Weinfurter H 1995 *Phys. Rev.* A **52** 3457
[13] Knill E, Laflamme R and Milburn G J 2001 *Nature* (London) **409** 46
[14] Koashi M, Yamamoto T and Imoto N 2001 *Phys. Rev.* A **63** 030301
[15] Gottesman D and Chuang I L 1999 *Nature* (London) **402** 390
[16] Pittman T B, Jacobs B C and Franson J D 2001 *Phys. Rev.* A **64** 062311
[17] Yurke B and Stoler D 1992 *Phys. Rev.* A **46** 2229
[18] Raussendorf R and Briegel H J 2001 *Phys. Rev. Lett.* **86** 5188
[19] Raussendorf R, Browne D E and Briegel H J 2003 *Phys. Rev.* A **68** 022312
[20] Gottesman D 1996 *Phys. Rev.* A **54** 1862
Schlingemann D and Werner R F 2001 *Phys. Rev.* A **65** 012308
[21] Gühne O, Tóth G, Hyllus P and Briegel H J 2005 *Phys. Rev. Lett.* **95** 120405
[22] Lu C Y, Zhou X Q, Gühne O, Gao W B, Zhang J, Yuan Z S, Goebel A, Yang T and Pan J W 2007 *Nature Physics* **3** 91
[23] Henny M, Oberholzer S, Strunk C, Heinzel T, Ensslin K, Holland M and Schönenberger C 1999 *Science* **284** 296
[24] Oliver W D, Kim J, Liu R C and Yamamoto Y 1999 *Science* **284** 299
[25] Lafarge P, Pothier H, Williams E R, Esteve D, Urbina C and Devoret M H 1991 *Z. Phys.* B **85** 327
[26] Field M, Smith C G, Pepper M, Ritchie D A, Frost J E F, Jones G A C and Hasko D G 1993 *Phys. Rev. Lett.* **70** 1311
[27] Molenkamp L W, Flensberg K and Kemerink M 1995 *Phys. Rev. Lett.* **75** 4282